Chemosphere 120 (2015) 615–620

Contents lists available at ScienceDirect

Chemosphere

journal homepage: www.elsevier.com/locate/chemosphere

# Adsorption kinetics of pesticide in soil assessed by optofluidics-based biosensing platform

Feng Long [a,*], Anna Zhu [b], Hanchang Shi [c], Jianwu Sheng [c], Zhen Zhao [c]

[a] School of Environment and Natural Resources, Renmin University of China, Beijing, China
[b] Department of Chemistry, Massachusetts Institute of Technology, Cambridge, MA, USA
[c] State Key Joint Laboratory of ESPC, School of Environment, Tsinghua University, Beijing, China

## HIGHLIGHTS

- Optofluidic biosensor was firstly used for adsorption kinetics assay of pesticides.
- The platform shows unique advantages for investigation of adsorption kinetics in soil.
- The platform is sensitivity, rapidity, small sample volume, and cost-effective.
- A simple and green method used to investigate transport mechanism of trace analytes.

## ARTICLE INFO

*Article history:*
Received 7 March 2014
Received in revised form 19 September 2014
Accepted 20 September 2014

Handling Editor: Tamara S. Galloway

*Keywords:*
Optofluidics
Biosensor
Adsorption kinetics
Fluorescence immunoassay
Atrazine

## ABSTRACT

The adsorption of pesticides in soil is a key process that affects transport, degradation, mobility, and bioaccumulation of these substances. To obtain extensive knowledge regarding the adsorption processes of pesticides in the environment, the new green assay technologies for the rapid, sensitive, field-deployable, and accurate quantification of pesticides are required. In the present study, an evanescent wave-based optofluidics biosensing platform (EWOB) was developed by combining advanced photonics and microfluidics technology for the rapid sensitive immunodetection and adsorption kinetics assay of pesticides. The robustness, reusability, and accuracy of the EWOB allow an enhanced prediction of pesticide adsorption kinetics in soil. Using atrazine (ATZ) as the target model, we found that the adsorption kinetics in soil followed a pseudo-second-order kinetic model. EWOB was compared with liquid chromatography–mass spectrometry/mass spectrometry (LC–MS/MS) method and yielded a good correlation coefficient ($r^2$ = 0.9968). The underestimated results of LC–MS/MS resulted in a higher adsorption constant of ATZ in soil derived from LC–MS/MS than that of a biosensor. The proposed EWOB system provides a simple, green, and powerful tool to investigate the transport mechanism and fate of pesticide residues.



## 1. Introduction

Pesticides have been used at increasing amounts to improve agricultural production and yield for 50 years (Hou et al., 2003; Graziano et al., 2006; Katsumata et al., 2006; Zacco et al., 2006; Pichetsurnthorn et al., 2012). The increasing amounts of these contaminants in various natural water systems and in agriculture products have caused increasing concerns because of the adverse effects of these substances on aquatic ecosystems and non-target organisms (Graziano et al., 2006). Previous studies demonstrated that the adsorption processes of pesticides in soil is of great importance because this procedure affects other processes, such as transport, degradation, mobility, and bioaccumulation (Singh et al., 2004; Liu et al., 2010). All of these processes greatly determine the risk of pesticide contaminating surface water and groundwater. Therefore, the extensive knowledge of the adsorption characteristics of pesticides in soil is necessary to predict the transformation and fate of these substances in the environment and protect water bodies from pesticide contamination (Flores et al., 2009; Siripattanakul et al., 2009). Analytical technologies are keys to obtaining accurate information regarding adsorption. Traditional analytical methods such as high-performance liquid chromatography (Katsumata et al., 2006), liquid chromatography–mass spectrometry (LC–MS) (Pichetsurnthorn et al., 2012), and gas chromatography with mass spectrometry identification (Hou et al., 2003) require complicated and time consuming pre-treated procedures (e.g., extraction and concentration). In addition, these

* Corresponding author.
*E-mail address:* longf04@ruc.edu.cn (F. Long).

http://dx.doi.org/10.1016/j.chemosphere.2014.09.072
0045-6535/

methods are difficult to apply in field investigation. During these pre-treated processes, toxic reagents have to be used (Hou et al., 2003; Katsumata et al., 2006; Pichetsurnthorn et al., 2012). Furthermore, a part of the target that should be measured may be lost and transformed, thereby leading to underestimated results. Hence, new green assay methods should be developed for the rapid, inexpensive, field-deployable, sensitive and accurate pesticide quantification with minimal sample and reagent volumes.

Optofluidics-based biosensing platform is a synergistic integration of photonics, microfluidics, and biosensor technologies; this platform also represents one of the most significant and active advances in biological/chemical analysis that provides numerous unique characteristics to enhance the sensing performance and simplify microsystem design (Psaltis et al., 2006). Many optical properties, such as fluorescence, refractive index, Raman scattering, absorption and polarization, can be exploited individually or in combination to generate sensing signals (Fan and White, 2011). The majority of optical waveguides (e.g., optic fiber) operate based on total internal reflection (TIR); in addition, the evanescent wave generated at optical waveguide surfaces penetrates the surrounding solution of lower refractive index and decays exponentially with distance (Psaltis et al., 2006; Fan and White, 2011). Microfluidics devices can function with small sample and reagent consumption, low unit costs, shorter reaction times, and parallel operation; these advances may possibly lead to the integration a whole laboratory in a chip (Thorsen et al., 2002). Microfluidics is not only an add-on accessory to an optofluidics device, but also an integral part of this system (Harazim et al., 2012). Therefore, optofluidics is suitable for biological/chemical detection in extremely small detection volumes (femtoliters to nanoliters) (Psaltis et al., 2006; Harazim et al., 2012).

In the current study, an evanescent wave-based optofluidics biosensor platform (EWOB) was developed to conduct a rapid on-site determination of pesticides by combining the evanescent wave fiber optic biosensor and microfluidics technology. A microcosm was prepared to investigate pesticide adsorption. Kinetic experiments were performed to provide further insights into pesticide adsorption. Atrazine [6-chloro-N-ethyl-N-1-(1-methylethyl)-1,3,5-triazine-2,4-diamine, ATZ], which is one of the most heavily used herbicides worldwide, was selected as a model target (Katsumata et al., 2006). ATZ is a putative endocrinal disruptor that poses a potential health risk to humans and wildlife even at very low levels (Graziano et al., 2006; Katsumata et al., 2006; Zacco et al., 2006). ATZ is routinely detected in various natural water systems, including groundwater and surface water, because of moderate solubility and relative persistence (Katsumata et al., 2006; Ionescu et al., 2010). The US Environmental Protection Agency (USEPA) has classified ATZ as a possible human carcinogen and mandated a drinking water standard limit of 3 $\mu g\,L^{-1}$ (Stoker et al., 2002). The proposed optofluidics biosensing system shows a considerable promise to conduct an on-site detection of pesticides and investigate the transport mechanism of pesticides by using a simple, fast, and portable technology.

## 2. Experimental

### 2.1. Chemicals and reagents

Bovine serum albumin (BSA), 3-aminopropyl triethoxysilane (APTS), glutaraldehyde, N,N′-Dicyclohexylcarbodiimide (DCC), N-hydroxysuccinimide (NHS), Atrazine (ATZ), N,N-Dimethylformamide (DMF), 3-mercaptopropionic acid (MPA), sodium dodecyl sulfate (SDS), 2,4-Dichlorophenoxyacetic acid (2,4-D), Bisphenol A, Diuron, and Simazine were purchased from Sigma–Aldrich (Steinheim, Germany). All other reagents, unless otherwise specified, were supplied by the Beijing Chemical Agents; they were also analytical grade and used without further purification. Distilled deionized water was used throughout the investigation. About 1 mg $mL^{-1}$ atrazine stock solutions were prepared in 0.01 M phosphate-buffered saline (PBS) and stored at 4 °C. Standard concentrations of the analyte were prepared from the stock solution by serial dilutions in 0.01 M PBS.

Anti-ATZ monoclonal antibody (Anti-ATZ-MAb) was produced by our research group and labeled by Cy5.5 as previously described (Long et al., 2009).

### 2.2. Preparation of mercaptopropionic acid derivative of ATZ (MPAD) and ATZ-BSA

MPAD and the hapten conjugate ATZ-BSA (Fig. S1) was synthesized similar to the procedure proposed by Goodrow et al. (Goodrow et al., 1990). Briefly, 4.6 mmol of ATZ was slowly added into 50 mL of ethanol under constant stirring. Then, 2.0 g KOH was added before 4.7 mmol of MPA in ethanol solution was added. After the mixture was refluxed for 3 h, another 4.7 mmol of MPA was added. The mixture was further refluxed for 3 h, and the solvent was dried under rotary evaporation. The residue was taken up in 25 mL of 5% $NaHCO_3$ and washed thrice with 10 mL of chloroform. The aqueous layer of the solution was acidified (pH 2.0) with 6 N HCl, causing the acidic derivative to precipitate immediately. The supernatant was decanted, and the derivative was dried under rotary evaporation. The precipitate was further dissolved in 1 mL of ethanol and then allowed under reduced pressure at 37 °C to form MPAD crystals. The product was stored in a tightly sealed bottle for further use. To synthesize the hapten conjugate ATZ-BSA, 0.2 mmol of the MPAD derivative of ATZ and 0.2 mmol of NHS were added in 2 mL of DMF. Then, 0.2 mmol DCC in 0.5 mL DMF was added. The mixture was incubated for 18 h at room temperature (RT) and then centrifuged for 5 min at 10,000 rpm to remove the urea precipitate. The reaction mechanism of MPAD protein conjugation is shown in Fig. S1. The supernatant (1 mL) was added dropwise into 5 mL 75 mg BSA solution (PBS, pH 7.4) and stirred for 4 h at 4 °C. The conjugates were passed through P10 gel filtration column (Pharmacia, Sweden). The fractions with maximum protein concentration were collected, pooled, and checked for the final concentration of protein (hapten-protein) using a UV spectrophotometer at 280 nm. The estimated number of hapten molecules attached to the carrier protein (hapten-to-protein molar ratio) BSA was 18.

### 2.3. Modification of fiber optic sensor

Details on the modification of the combination tapered fiber optic sensor were described previously (Long et al., 2009). The hapten-carrier conjugate ATZ-BSA used as a recognition element was covalently attached onto the sensing surface of the fiber optic sensor by the glutaraldehyde-covalent-coupling strategy to assure the reusability of the sensor surface without affecting the binding properties of the immobilized molecule (Fig. S2) (Hofstetter et al., 1999). Prior to surface modification, the fiber optic sensor surface was cleaned with a piranha solution [$H_2SO_4/H_2O_2$, 3:1 (v/v)] for 30 min, rinsed with ultrapure water, and then dried in an oven at 105 °C. The immobilization of ATZ-BSA onto the surface of the fiber optic sensor is illustrated in Fig. S2. The fiber optic sensor was first aminated by immersion in 2% (v/v) APTS acetone solution for 1 h to coat a reactive silane layer with an aminated-terminal silane. Excess APTS was eliminated with acetone to ensure order and uniformity of the self-assembled monolayer. The sensor was first immersed in a 5.0% (v/v) glutaraldehyde solution for 1 h at 37 °C, washed with water, and then immersed overnight in 1 mL of a 0.5 μM ATZ-BSA in PBS solution (pH 7.4) at 4 °C to immobilize ATZ-BSA onto the surface of aminated-silanized

sensor. To block non-specific binding sites on the sensor, the sensor was immersed for 20 min in 2 mg $mL^{-1}$ BSA.

### 2.4. EWOB platform

In the present study, the EWOB system comprises three parts, namely, a microfluidics system, an integrated optical system, and an embedded computer system (Fig. S3) (Long et al., 2014). The microfluidics system consisted of a poly (methyl methacrylate) (PMMA) microfluidics chip and a peristaltic pump. The PMMA microfluidics device was fabricated by laser ablation[21] combined with electroplating and hot embossing (Suzhou Wenhao Biochip Co., China). The combination tapered fiber optic sensor (effective part = 15 mm length × ∅220 μm) was embedded into the microfluidics channel with the following dimensions: 15 mm in length, 500 μm in width, and 500 μm in height.

The optical sub-system of the optofluidics system should function (1) to deliver laser light to a well-defined biosensing assay zone and (2) to collect fluorescent light from the biosensing assay zone. This sub-system can also transmit the fluorescence light to an optical filter to be separated from scattered laser light prior to electronic detection. The design investigated in the present study uses an integrated single-multi-mode fiber optic coupler to transmit excitation laser and collet fluorescence signal for the same purpose. Light from a pulse laser (2 kHz) with a wavelength of 635 nm and a power of 5 mW was directly launched into the single-mode fiber of the single multi-mode silica fiber optic coupler. Laser light then entered the multi-mode fiber with a diameter of 600 μm and a numerical aperture of 0.22 from the single-mode fiber. The excitation light from the laser was then coupled to a combination tapered fiber optic sensor by using a fiber connector. The incident light was propagated along the entire length of the fiber optic sensor via TIR. The evanescent wave was generated at the fiber optic sensor surface. This evanescent wave then interacted with the surface-bound fluorescent-labeled analyte complexes, which excited the fluorophores. The collected fluorescence signal was filtered using a bandpass filter (FF01-692/40, Semrock, USA) to reject any lost and scattered laser light. This signal was subsequently monitored using a photodiode by digital lock-in detection. The optofluidics platform can be suitable to detect pollutants rapidly at field sites by reducing optical components and unnecessary optical alignment. Furthermore, light transmission efficiency increased, light loss decreased, and signal-to-noise (S/N) ratio improved (Long et al., 2009). All of the reagents were delivered using a flow delivery system operated using a peristaltic pump. The fluid delivery system control, data acquisition, and data processing were automatically performed by the embedded computer. All of the assay-relevant parameters were controlled using a special parser embedded in the user interface of the measurement software.

### 2.5. Adsorption kinetics of ATZ on soil

To investigate the adsorption kinetics of ATZ on soil, we prepared one microcosm in 250 mL of conical flak using 2.5 g of soil (from Tsinghua Campus of Beijing, China) and 150 mL of pure water. After the soil and water were mixed, 10 mL of 150 μg $mL^{-1}$ ATZ was added to the microcosm. The experiments were conducted using an orbital shaker at 100 rpm for a period of 24 h at room temperature (25 °C). Before sampling was conducted, the mixture was deposited 5 min, and 200 μL of samples were collected from the supernatant at different time intervals (0, 0.5, 1, 2, 4, 6, 12, and 24 h) for biosensor and LC–MS/MS analyses. LC–MS/MS detection was performed according to USEPA method 536 (USEPA, 2007). After the supernatant was simply filtered using 0.22 μm filters, the ATZ concentration in the samples was detected using the optofluidics-based biosensor.

### 2.6. Data evaluation

A pseudo-first-order and pseudo-second-order equations have been widely used to predict adsorption kinetics. In terms of boundary conditions $q = 0$ at $t = 0$ and $q = q_e$ at $t = t$, the pseudo-first-order adsorption kinetic model proposed by Langergren and Svenska (1898) is defined as follows:

$$\ln(q_e - q_t) = \ln q_e - k_a t \tag{1}$$

where $q_e$ and $q_t$ (mg $g^{-1}$) are the amounts of ATZ adsorbed at equilibrium and at time $t$ (h), respectively. $k_a$ (1/h) is the adsorption rate constant. The ATZ uptake at any time, $q_t$, was calculated using Eq. (2):

$$q_t = \frac{(C_0 - C_t)V}{W} \tag{2}$$

where $C_0$ and $C_t$ (mg $L^{-1}$) is the ATZ concentration in the solution at initial time and at any time, $t$ (h), respectively. We can obtain the $q_e$ by replacing $C_t$ in Eq. (2) with the ATZ concentration in the solution at equilibrium ($C_e$).

The pseudo-second-order equation (Ho and McKay, 1998) based on equilibrium adsorption was expressed as follows:

$$\frac{t}{q} = \frac{1}{k_a' q_e^2} + \frac{1}{q_e} t \tag{3}$$

where $k_2'$ (g $mg^{-1}$ h) is the rate constant of second-order adsorption.

## 3. Results and discussion

### 3.1. Characterization of optofluidics-based sensor

Using glutaraldehyde coupling strategy, we covalently immobilized ATZ-BSA onto an aminated fiber optical sensor surface (Fig. S2). This crosslinker was conjugated between the amino groups of silanization reagents immobilized onto the fiber optic sensor surface and the epsilon amino group of BSA. Several control experiments were conducted to confirm that the observed fluorescence signal originated from the binding between ATZ immobilized onto the sensor surface and Cy5.5-labeled anti-ATZ-MAb (Fig. S4). These results showed that the combination tapered fiber optic sensor exhibited a high capability to detect the binding kinetics between small molecules and the corresponding specific antibody. In this detection process, the minimal free fluorescence in the solution was excited, and the non-specific adsorption of antibody onto the fiber optic sensor surface was also negligible.

The selectivity of the sensor was also assessed by evaluating the responses to potential interference from other pesticides such as 2,4-D, diuron, and simazine, as well as other chemicals including BPA, microcystin-LR and estriol at 200 μg $L^{-1}$ (Fig. S5). The results showed that the anti-ATZ MAb developed by our group exhibits high specificity to ATZ, without uniquely binding to the other pesticides and chemicals tested. This selectivity is a key factor affecting the ability of this biosensor to detect environmental pollutants without separation.

The stability and activity of an ATZ conjugate immobilized sensor surface were evaluated by a series of immunoassays (data not shown). After each ATZ determination cycle, the non-covalently bound antibody was completely removed, and the active sensor surface was regenerated using 0.5% sodium dodecyl sulfate (SDS) solution (pH 1.9). The sensor surface can be reused for more than 100 measurements without damaging the physical–chemical properties. The storage stability of the fiber optic sensor was examined for 90 d. The sensor retained approximately 85% of the original response after 90 d of storage. This result indicated that the stability and robustness of the conjugates immobilized onto the sensor

were higher than those of the other immunoassays (e.g., ELISA) reported for ATZ (Graziano et al., 2006; Pichetsurnthorn et al., 2012; Zacco et al., 2006). The reusability and stability of the proposed biosensor ensure the cost-effectiveness and accuracy of ATZ measurement.

### 3.2. ATZ detection using the EWOB system

Fig. 1 illustrates the sensing quantification mechanism of the EWOB for the indirect competitive immunoassay of ATZ. To detect the ATZ, we pre-reacted 0–200 μg $L^{-1}$ of ATZ solutions with 1.2 nM fluorescence-labeled anti-ATZ-MAb for 5 min. A high ATZ concentration in the sample corresponded to numerous binding sites of occupied antibodies. The mixture was then delivered to the optofluidics cell at a flow-rate of 30 μL $min^{-1}$ for 30 s. The EWOB system recorded the time-dependent fluorescence signal when the antibodies with the remaining binding sites bound to ATZ-BSA conjugates immobilized onto the sensor surface (Fig. 2A). The fluorescence signal rapidly increased initially when the sample was introduced. After 5 min, the growth rate of fluorescence signal decreased. We observed that the fluorescence signal still increased and reached a plateau after 25 min. In terms of the reduction of testing time, the signal value of 9 min, which is approximately 75% of the maximum, was considered as the effective result. The increasing amount of ATZ introduced to the mixture inhibited the antibody binding to the immobilized binding partner. This change also induced proportional decrements in the fluorescence signal. No obvious fluorescent signals could be observed when the ATZ flow was >200 μg $L^{-1}$. This observation further showed that fluorescent signals were not obtained by either non-specific adsorption of Cy5.5-labeled anti-ATZ-MAb on the sensor surface or excitation of free Cy5.5-labeled anti-ATZ-MAb in the solution. To regenerate the sensor surface, we introduced 0.5% SDS solution (pH 1.9) for 120 s. The sensor was washed with PBS solution to remove regeneration solution.

Fig. 2B shows that the dose–response curve of the detected ATZ was normalized by expressing the signal of each standard point as the ratio to the signal of the blank sample without ATZ. The experimental results were fitted to a four-parameter logistic equation (Supporting Information). The limit of detection (LOD) was 0.06 μg $L^{-1}$ for ATZ as obtained from the calibration curve based on an S/N ratio of 3. The linear response of the sensor to quantify ATZ ranged from 0.45 μg $L^{-1}$ to 75 μg $L^{-1}$, with relative standard deviations <5.97%. The LOD of the sensor satisfied the requirement for the determination of ATZ in drinking water as imposed by USEPA (2007). The detection limit we obtained initially is highly comparable to those described in the previous studies (Table S1). High sensitivity can be attributed to the following reasons. First, the surface chemistry of the ATZ-OVA conjugates on the sensor surface maintained the activity of the immobilized ATZ toward anti-ATZ-MAb. This property also diminished non-specific adsorption. Second, a high number of hapten molecules attached to each carrier protein allowed numerous fluorescence-labeled antibodies to bind to the sensor surface and less antibody concentration was used. For a competitive immunoassay, lower reagent concentrations (e.g., fluorescence-labeled antibody) favored an effective analyte competition, resulting in higher sensitivity (Long et al., 2014). Third, in contrast to conventional analytical methods, the proposed optofluidics-based biosensor used to detect ATZ requires no complicated sample pre-treated processes; instead, only a small amount of sample volume (<5.0 μL) is necessary. In addition, sensor surface regeneration occurs without compromising immunoreactivity for multiple analyses and is essential for practical applications.

### 3.3. Comparison between biosensor and LC–MS/MS

To evaluate the matrix effects on the EWOB system and its on-site detection ability, the supernatants in the microcosm were taken out and spiked with ATZ at concentrations of 2, 5, 20, and 50 μg $L^{-1}$, respectively. These samples were simultaneously measured by EWOB system and chromatographic method. The results were summarized in Table S2. A comparison between these two methods yielded good correlation results ($y = 0.8214x - 0.3760$). The slope (0.8214) of the linear regression equation indicated that the LC–MS/MS results were slightly less than the biosensor-measured values. We assumed that some ATZ losses and/or transformations were unavoidable during the complicated sample pre-treatment in LC–MS/MS detection, which led to the underestimated results. However, the correlation coefficient ($r^2 = 0.9968$) demonstrated satisfactory agreement between the methods. These results indicated that the EWOB system can be used for rapid, on-site, real-time measurements of ATZ in natural water sources.

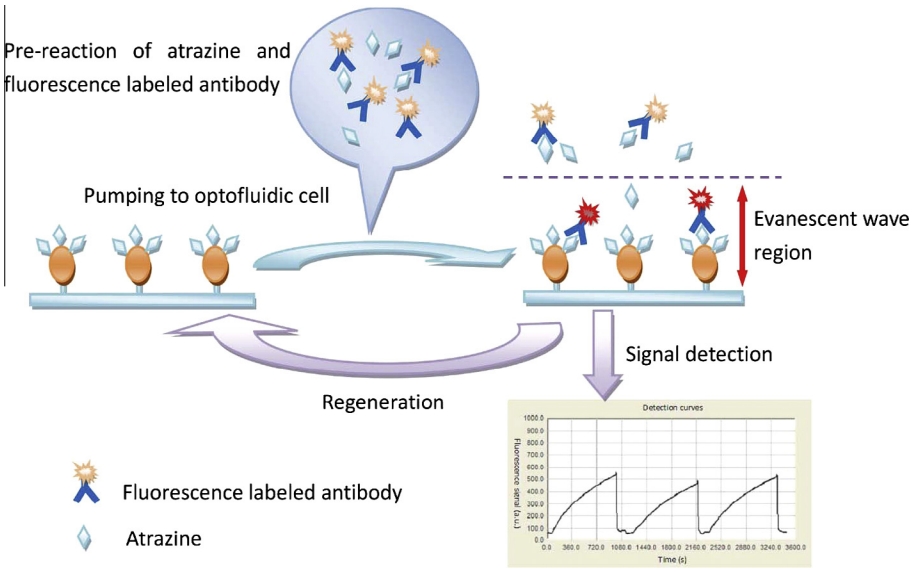


**Fig. 1.** Schematic of the sensing mechanism of ATZ detection.

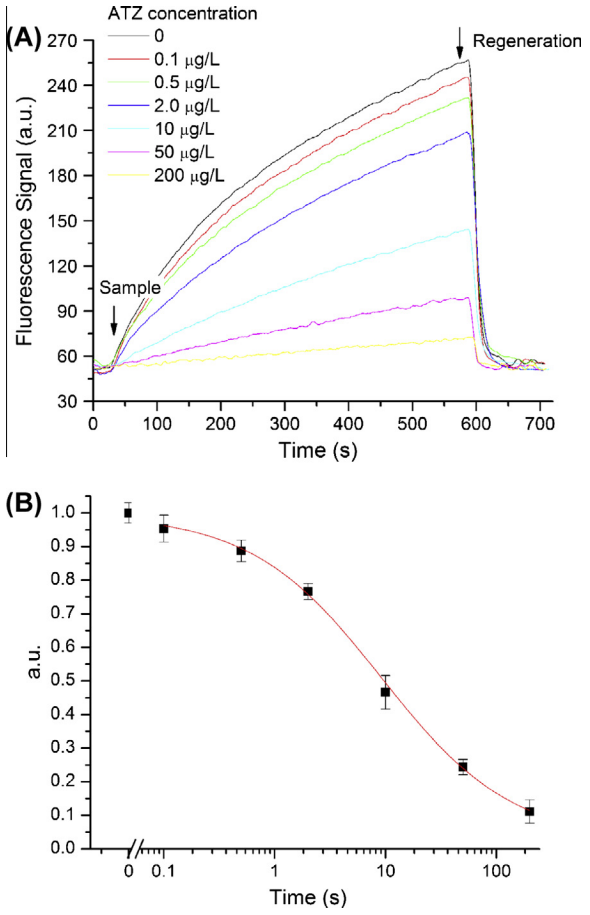


**Fig. 2.** (A) EWOB signal trace observed in the flow of the mixture of 1.2 nM Cy5.5-anti-ATZ-MAb and ATZ solution at various concentrations over the ATZ-BSA-modified fiber sensor surface. (B) Logarithmic calibration plot to determine ATZ using the EWOB system. The error bars in the figure correspond to the standard deviation of the data points in triplicate experiments. The results revealed that the standard deviation of the data points was within 8%.

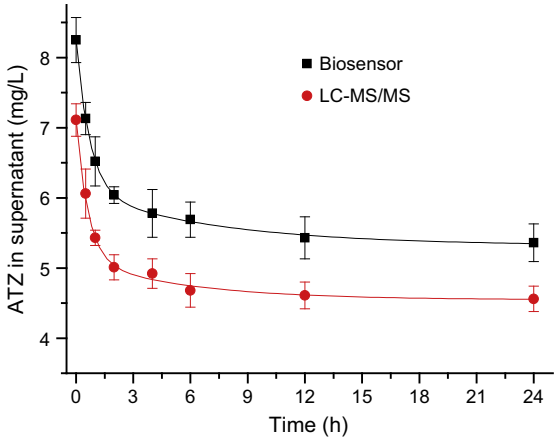


**Fig. 3.** ATZ adsorption kinetics in the microcosm obtained using optofluidics-based biosensor and validation by LC–MS/MS. Inset: Linear correlation between the optofluidics-based biosensor and LC–MS/MS.

### 3.4. Adsorption kinetics of ATZ in soil

Although the initial ATZ concentration was approximately 10 mg $L^{-1}$, the concentration of the first sample was only 8.25 and 7.11 mg $L^{-1}$ as indicated by biosensor and LC–MS/MS, respectively

**Table 1**
Pseudo-first-order and pseudo-second-order model equation constants and correlation coefficients for ATZ adsorption based on the detection results of biosensor and LC–MS/MS.

| Detection methods | $q_{e,exp}$ (mg $g^{-1}$) | Pesudo-first-order kinetic model | | | Pesudo-second-order kinetic model | | |
|---|---|---|---|---|---|---|---|
| | | $q_{e,exp}$ (mg $g^{-1}$) | $k_a$ (1/ h) | $R^2$ | $q_{e,exp}$ (mg $g^{-1}$) | $k'_a$ (1/ h) | $R^2$ |
| Biosensor | 0.2784 | 0.132 | 0.2594 | 0.9661 | 0.2811 | 9.318 | 0.9996 |
| LC–MS/MS | 0.3264 | 0.102 | 0.2973 | 0.9149 | 0.3289 | 14.076 | 0.9998 |

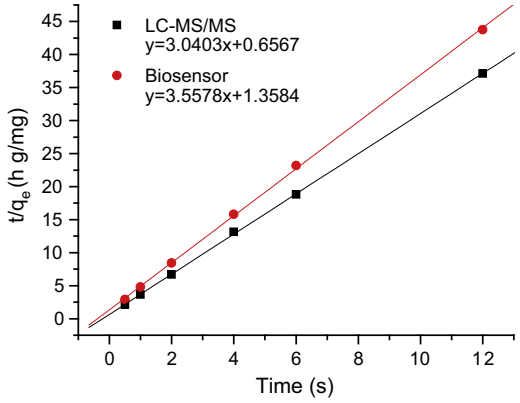


**Fig. 4.** Pseudo-second-order kinetics for ATZ adsorption in soil (room temperature) based on the detection results of biosensor and LC–MS/MS.

(Fig. 3). The adsorption kinetics exhibited the preliminary phase of rapid sorption and reached a steady state within a short period of 4 h in soil. After this stage, <7% variation in ATZ concentration in the soil was observed after 20 h. Considering solubility and hydrophobicity, we assumed that the vacant sites in the soil particles were filled within the first few hours. Pesticides then slowly migrated and diffused. Similar results have been reported for pesticide sorption in various adsorbents (Kumar and Philip, 2006; Hameed et al., 2008; Wang and Keller, 2009; Kumar and Singh, 2013).

The kinetic parameters provide important information regarding the adsorption rate prediction of ATZ uptake in soil. The kinetics of the adsorption data were investigated using pseudo-first-order and pesudo-second-order models as given in Eqs. (1) and (2), respectively. $k_a$ and $R^2$ for the pseudo-first-order kinetic model calculated from the plot of $\ln(q_e - q_t)$ versus $t$ (figure not shown) for LC–MS/MS and biosensor are listed in Table 1, respectively. The relatively small $R^2$ value as well as the disagreement between the experimental $q_e$ and the calculated value obtained from the linear plot demonstrated that ATZ adsorption in soil is not a first-order reaction.

Fig. 4 shows the plots of the pseudo-second-order kinetic of ATZ adsorption in soil based on the detection results of biosensor and LC–MS/MS. The linear plot of $t/q_t$ versus $t$ gave $1/q_e$ as the slope and $1/k'_a q_e^2$ as the intercept. The calculated $R^2$ and predicted equilibrium uptakes of the pseudo-second-order kinetic model are also listed in Table 1. Both detection methods show a good agreement between the experimental and calculated $q_e$ values. In Fig. 4, fitting was conducted by estimating the parameter values, which were continually optimized until the residual sum of squares showed no further significant decrease. The experimental data and the modeled curve (Fig. 4, red[1] line for LC–MS/MS results and black line for biosensor results) derived from pseudo-second-order equation were

[1] For interpretation of color in Fig. 4, the reader is referred to the web version of this article.

in good agreement. These results indicated that the pseudo-second-order model can likely predict ATZ adsorption in soil. Previous studies also found that the adsorption of pesticides from aqueous solutions in soil and high specific area-activated materials follows the pseudo-second-order kinetics (Kumar and Philip, 2006; Hameed et al., 2008; Salman and Hameed, 2010). $q_t$ and $q_e$ is higher than the true adsorption amount of ATZ in soil according to Eq. (2) because the results of LC–MS/MS were underestimated. Therefore, the adsorption constant derived from the LC–MS/MS results is higher than that of the biosensor.

## 4. Conclusion

Combining advanced photonics and microfluidics technology, we developed a EWOB platform for the rapid on-site detection and adsorption kinetics assay of pesticides. The field-based biosensor analysis results exhibit good correlation with laboratory-based conventional analytical methods. The robustness, reusability, and accuracy of this platform are accounted for an improved prediction method of pesticide adsorption kinetics in soil. This biosensing platform also shows unique advantages for the investigation of the pesticides adsorption kinetics. First, the indirect competitive immunoassay of ATZ using the EWOB system in water samples showed good characteristics, such as high sensitivity, rapidity, small sample volume, simplified manipulation, portability, reusability, and cost-effectiveness. Second, biosensing technology only requires simple pre-treatment process, ensuring an accurate detection result. Third, optofluidic-based biosensor is an environmentally-friendly detection method, in which no toxic reagents are required and minimum wastewater is produced. Therefore, the proposed EWOB system provides a simple, green, and powerful tool that can be used to investigate the transport mechanism and fate of pesticide residues.

## Acknowledgements

This research was financially supported by the National Natural Science Foundation of China (21077063, 21277173), the National Instrument Major Project of China (2012YQ3011105), and the Basic Research funds in Renmin University of China from the central government (13XNLJ01).

## Appendix A. Supplementary material

Supplementary data associated with this article can be found, in the online version, at http://dx.doi.org/10.1016/j.chemosphere.2014.09.072.

## References

Fan, X., White, I.M., 2011. Nat. Photon. 5, 591–597.
Flores, C., Morgante, V., González, M., Navia, R., Seeger, M., 2009. Chemosphere 74, 1544–1549.
Goodrow, M.H., Harrison, R.O., Hammock, B.D., 1990. J. Agric. Food Chem. 38, 990–996.
Graziano, N., McGuire, M.J., Roberson, A., Adams, C., Jiang, H., Blute, N., 2006. Environ. Sci. Technol. 40, 1163–1171.
Hameed, B.H., Tan, I.A.W., Ahmad, A.L., 2008. Chem. Eng. J. 144, 235–244.
Harazim, S.M., Bolanös, V.A., Kiravittaya, S., Sanchez, S., Schmidta, O.G., 2012. Lab Chip 12, 2649–2655.
Ho, Y.S., McKay, G., 1998. Can. J. Chem. Eng. 76, 822–826.
Hofstetter, O., Hofstetter, H., Wilchek, M., Schurig, V., Green, B.S., 1999. Nat. Biotechnol. 17, 371–374.
Hou, L., Shen, G., Lee, H.K., 2003. J. Chromatogr. A985, 107–116.
Ionescu, R.R., Gondran, C., Bouffier, L., Jaffrezic-Renault, N., Martelet, C., Cosnier, S., 2010. Electrochim. Acta 55, 6228–6232.
Katsumata, H., Kaneco, S., Suzuki, T., Ohta, K., 2006. Anal. Chem. Acta 577, 214–219.
Kumar, M., Philip, L., 2006. Chemosphere 62, 1064–1077.
Kumar, A., Singh, S., 2013. J. Pet. Environ. Biotechnol. 4, 5.
Langergren, S., Svenska, B.K., 1898. Veternskapsakad Handlingar 24, 1–39.
Liu, Y., Xu, Z., Wu, X., Gui, W., Zhu, G., 2010. J. Hazard. Mater. 178, 462–468.
Long, F., He, M., Zhu, A.N., Shi, H.C., 2009. Biosens. Bioelectron. 24, 2346–2351.
Long, F., Zhu, A., Zhou, X., Wang, H., Zhao, Z., Liu, L., Shi, H., 2014. Biosens. Bioelectron. 55, 19–25.
Pichetsurnthorn, P., Vattipalli, K., Prasad, S., 2012. Biosens. Bioelectron. 32, 155–162.
Psaltis, D., Quake, S.R., Yang, C., 2006. Nature 422, 381–386.
Salman, J.M., Hameed, B.H., 2010. Desalination 256, 129–135.
Singh, P., Suri, C.R., Cameotra, S.S., 2004. Biochem. Biophys. Res. Commun. 317, 697–702.
Siripattanakul, S., Wirojanagud, W., McEvoy, J., Limpiyakorn, T., Khan, E., 2009. J. Appl. Microbiol. 106, 986–992.
Stoker, T.E., Guidici, D.L., Laws, S.C., Cooper, R.L., 2002. Toxicol. Sci. 67, 198–206.
Thorsen, T., Maerkl, S.J., Quake, S.R., 2002. Science 298, 580–584.
U.S. Environmental Protection Agency, 2007. METHOD 536: Determination of triazine pesticides and their degradates in drinking water by liquid chromatography electrospray ionization tandem mass spectrometry, October 2007. <http://www.epa.gov/ogwdw/methods/pdfs/methods/met536.pdf>.
Wang, P., Keller, A.A., 2009. Water Res. 43, 1448–1456.
Zacco, E., Pividori, M.I., Alegret, S., Galve, R., Marco, M.P., 2006. Anal. Chem. 78, 1780–1788.